Acoust. Sci. & Tech. **22**, 4 (2001)

PAPER

Analysis of an ultrasonic field attenuated by oscillating cavitation bubbles

Shinfuku Nomura[1] and Masafumi Nakagawa[2]

[1]*Department of Mechanical Engineering, Ehime University,*
3, Bunkyo-cyo, Matsuyama, 790–8577 Japan
e-mail: nomu@en1.ehime-u.ac.jp
[2]*Department of Mechanical Engineering, Toyohashi University of Technology,*
1–1, Hibarigaoka, Tempaku-cyo, Toyohashi, 441–8580 Japan

(*Received 14 August 2000, Accepted for publication 25 November 2000*)

Abstract: This paper numerically analyzes the sound pressure on an object in an ultrasonic cleaning vessel by considering the dissipation of cavitation bubbles. To clarify the effect of ultrasonic attenuation on the number of cavitation bubbles, the cavitation intensity on a brass object is measured experimentally by changing the quantity of water. Then, the analyzed sound pressure results are compared with the measured cavitation intensity results. The energy dissipation by the oscillation of bubbles is estimated by the irreversible process of heat and mass transfer. The calculation is carried out for the natural oscillation and forced oscillation of cavitation bubbles. It is found that the dissipation of thermal conduction results from the radial oscillation of bubbles by ultrasound. The sound pressure calculated by this dissipation agrees with the cavitation intensity profile estimated using experimental results from the erosion loss of aluminum foil. As the quantity of the water in the cleaning vessel is increased, the sound pressure becomes lower. This is because the amount of energy dissipation of the ultrasonic wave increases proportionally to the number of bubbles. However, when the standing wave causes resonance between the ultrasonic generator and the block, the effect of the sound pressure on the bottom of the block is not disturbed by the water volume.

Keywords: Ultrasonic, Cavitation bubble, Forced oscillation, BEM, Thermal diffusion, Energy dissipation

PACS number: 43.35.Ei

1. INTRODUCTION

By applying ultrasonic vibration to liquid, pressure fluctuation of a few atmospheres is easily caused, and as a result, cavitation bubbles are generated. The impulsive forces induced by the creation and collapse of these cavitation bubbles are utilized to clean various materials, as evidenced today by the widely used ultrasonic cleaners. In order to forecast accurate cleaning effects, it is necessary to obtain the sound pressure profiles of the cleaning liquid and surface of the object to be cleaned.

The authors have studied heat transfer enhancement by ultrasonic vibration and have clarified that moving cavitation bubbles agitate the thermal boundary layer on the heating surface and increase the heat transfer coefficient [1,2]. Ultrasonic cleaning and heat transfer enhancement are analogous phenomena in the sense that both utilize the effect of cavitation. We suppose that a large cleaning effect is obtained with a strong cavitation intensity. We also suppose that this cavitation intensity becomes largest at the point where the amplitude of the sound pressure is highest. To predict the effects of ultrasonic cleanering on various species of objects, it is necessary to accurately estimate the dissipation of cavitation bubbles in the cleaning vessel being employed because the sound pressure is governed by the attenuation of ultrasonic vibration.

The present study suggests a method to estimate an effect of cleaning theoretically, by analyzing the surface sound pressure on a block in a cleaning vessel while taking account of the dissipation of cavitation bubbles. Furthermore, the cavitation intensity on the block surface is measured while varying the quantity of water filling the cleaning vessel to clarify the effects of ultrasonic attenuation on the number of cavitation bubbles. The analyzed sound pressure results are compared with the measured cavitation intensity results.

2. SOUND ANALYSIS

The experimental apparatus is composed of a rectan-

gular block (to be cleaned) and an ultrasonic generator fixed to the bottom of the cleaning vessel as shown in Fig. 1. The outer dimensions of the block are 105 mm (width) × 105 mm (depth) × 190 mm (height), and brass is used as the specimen. The block is immersed in fluid with intentional shifting from the center. The main reason for this is to be able to investigate the state of the sound field for practical application in detail. The cleaning vessel is made of double-walled acrylic resin plates having dimensions of 370 mm (width) × 340 mm (depth) × 380 mm (height) for the inner frame, and it can maintain a constant water temperature. Later experiments used this cleaning vessel to measure cavitation intensity values.

A standard ultrasonic cleaner unit with an output electric power of 300–600 W variable is used as the ultrasonic generator and placed at the bottom part of the cleaning vessel. This generator unit is constructed with thirteen transducers having a resonant frequency of 40 kHz, and it can generate high intensity ultrasonic vibration all over the cleaning vessel.

This apparatus is simulated by a two-dimensional cleaning vessel as shown in Fig. 2. On the occasion of an analysis, the dimensionless variables of the x, y coordinates and sound pressure p are defined by using wavelength λ and the normal direction velocity of the vibrating plane of the generator υ_n.

$$\frac{x}{\lambda} \to x, \quad \frac{y}{\lambda} \to y, \quad k\lambda \to k(=2\pi), \quad \frac{p}{2\pi\rho c\upsilon_n} \to p \quad (1)$$

Here, k is the wave number, ρ is the density of the medium and c is the sound velocity. The boundary conditions are as follows: the velocity on the vibrating plane is fixed, the pressure on the acrylic wall is assumed to be zero as it is equal to the atmospheric pressure at the outer wall of the cleaning vessel, and the velocity on the brass block is assumed to be zero as a rigid body.

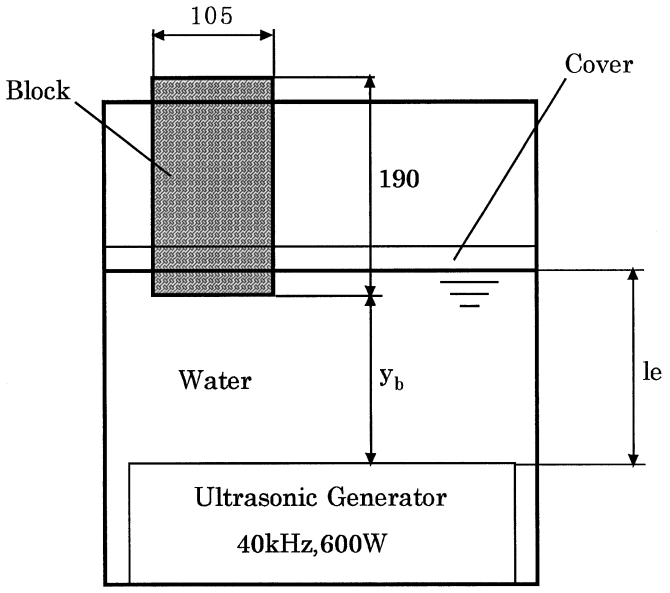

Fig. 1 Experimental apparatus.

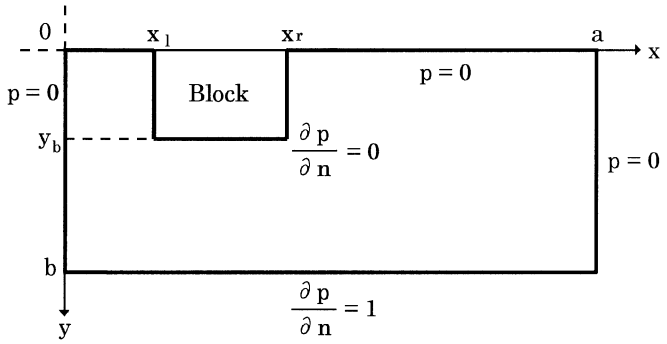

Fig. 2 Boundary condition.

The *Helmholtz* equation governing this field has to be solved to obtain information regarding the standing wave field.

$$(\nabla^2 + k^2)p(\boldsymbol{r}) = 0 \quad (2)$$

Since the sound field in the cleaning vessel is formed by forced oscillation by the addition of ultrasonic energy, the attenuation term has to be considered to estimate the finite amplitude of the sound pressure. Accordingly, the analysis of the sound field is performed by making the wave number k a complex expression [3]. When the cleaning vessel contains cavitation bubbles, it is almost impossible to evaluate the attenuation term because of the bubble oscillation. In the cleaning vessel, however, almost no ultrasonic vibration attenuation is conceivable due to the existence of the standing wave and the nearly 90° phase difference between velocity υ and pressure p. Accordingly, the analysis is practiced by giving k in Eq. (2) as a real number, and by estimating the attenuation later from the equation of motion of the cavitation bubbles. Finally, the sound pressure is calculated by connecting both solutions.

Equation (2) can be analyzed by the boundary element method, which results in the following boundary integral equation by means of *Green*'s function [4].

$$p(\boldsymbol{r}) = \int_S \{G(\boldsymbol{r}|\boldsymbol{r}')\ \mathrm{grad}\ p(\boldsymbol{r}') - p(\boldsymbol{r}')\ \mathrm{grad}'\ G(\boldsymbol{r}|\boldsymbol{r}')\} \cdot \boldsymbol{n}' dS'. \quad (3)$$

The term G represents *Green*'s function. Here, the prime denotes a point on the surface element dS', and therefore, $\boldsymbol{n}'$ is a normal unit vector to dS', $\boldsymbol{r}'$ is a position vector to dS', and $\mathrm{grad}'\ G(\boldsymbol{r}|\boldsymbol{r}')$ is the space differential of $G(\boldsymbol{r}|\boldsymbol{r}')$ with respect to $\boldsymbol{r}'$. A basic solution of *Green*'s function in two-dimensional analysis is given by the zero-order *Hankel* function.

$$G(\boldsymbol{r}|\boldsymbol{r}') = \frac{i}{4} H_0^{(1)}(k|\boldsymbol{r} - \boldsymbol{r}'|)$$

$$= -\frac{1}{4}N_0(k|\boldsymbol{r}-\boldsymbol{r}'|) + \frac{i}{4}J_0(k|\boldsymbol{r}-\boldsymbol{r}'|) \tag{4}$$

where N_0 and J_0 represent the zero-order *Neuman* function and *Bessel* function, respectively. Although a complex calculation has to be carried out to solve the boundary integral equation, the calculation can be effectively done by using the *Neuman* function when it is solved by making k a real number. By substituting Eq. (4) for *Green*'s function in Eq. (3) and putting the numerical integration into practice, the pressure on the boundary element can be obtained.

3. ENERGY DISSIPATION OF ULTRASONIC VIBRATION BY BUBBLES

The value υ_n, which is used in Eq. (1) to non-dimensionalize the basic equations, has to be determined so as to find the actual pressure in the cleaning vessel. It is assumed that the energy attenuation is made zero in the analysis developed in the previous section, and as a result, the sound pressure pattern in the cleaning vessel can be found. This assumption, however, makes it impossible to decide the absolute amplitude of the pressure wave. The actual pressure is determined by the mechanism of the energy attenuation in the cleaning vessel. There are a large number of cavitation bubbles in the cleaning vessel, and the pressure wave depends largely on the attenuation induced by these bubbles. Here, the radial oscillation of the bubbles, which exerts both free oscillation and forced oscillation by ultrasonic vibration, is investigated by solving the governing equation of the dynamics of the bubbles, thermal conduction, and diffusion in the liquid phase and gas phase, when both evaporation and condensation occur. Since the cavitation bubbles generated by ultrasonic vibration are very small, simulation is performed by using a single bubble. Finally, the attenuation of all of these single bubbles is integrated over the volume of the vessel.

3.1. Governing Equation

The governing equation, which describes the phenomena occurring in the bubble, and the liquid surrounding it, induced by considering evaporation and condensation of vapor and the dissolution and precipitation of air at the bubble interface. The conservation equations for the gas phase (such as the continuity, the balance of the momentum, the energy conservation, and the diffusion equation) are given as follows.

$$\frac{\partial \rho_g}{\partial t} + \frac{1}{r^2}\frac{\partial}{\partial r} r^2 \rho_g \upsilon_r = 0 \tag{5}$$

$$\rho_g \frac{\partial \upsilon_r}{\partial t} + \rho_g \upsilon_r \frac{\partial \upsilon_r}{\partial r} = -\frac{\partial p_g}{\partial r} \tag{6}$$

$$\rho_g\left(\frac{\partial h_g}{\partial t} - \frac{1}{\rho_g}\frac{\partial p_g}{\partial t}\right) + \rho_g \upsilon_r\left(\frac{\partial h_g}{\partial r} - \frac{1}{\rho_g}\frac{\partial p_g}{\partial r}\right) = \lambda_g \Delta T_g \tag{7}$$

$$\frac{\partial \rho_v}{\partial t} + \frac{1}{r^2}\frac{\partial}{\partial r} r^2 \rho_v \upsilon_r = D_{av}\rho_g \Delta \frac{p_v M_v}{p_v M_v + p_a M_a} \tag{8}$$

where

ρ_g, ρ_v:	density of gas, vapor	(kg/m^3)
υ_r:	radial direction velocity	(m/s)
h_g:	specific enthalpy of gas	(J/kg)
λ_g:	heat conductivity of gas	(W/mK)
T_g:	temperature of gas	(K)
D_{av}:	diffusion coefficient of air into vapor	(m^2/s)
M_a, M_v:	molecular weight of residual gas in a bubble, vapor	(kg)

In each equation, p_g is the pressure in the bubble, which is the sum of two partial pressures of vapor and air,

$$p_g = p_v + p_a, \quad \rho_g = \rho_v + \rho_a \tag{9}$$

and h_g in Eq. (7) is the enthalpy of gas, which is given by

$$h_g = C_{pg}T_g = \frac{p_v M_v C_{pv} + p_a M_a C_{pa}}{M_a p_a + M_v p_v} T_g \tag{10}$$

In the liquid phase, the thermal conduction equation for the liquid phase around the bubble, the diffusion equation of air into liquid, and the equation of the motion of the bubble are given, respectively, as follows.

$$\rho_l C_l \frac{\partial T_l}{\partial t} = \lambda_l \Delta T_l \tag{11}$$

$$\frac{\partial \rho_{al}}{\partial t} = D_{al}\Delta \rho_{al} \tag{12}$$

$$\rho_l R\frac{d^2R}{dt^2} + \frac{3}{2}\rho_l\left(\frac{dR}{dt}\right)^2 + \frac{4\mu_l}{R}\frac{dR}{dt} = p_g - p_\infty - \frac{2\sigma}{R} \tag{13}$$

where

ρ_l:	density of liquid	(kg/m^3)
ρ_{al}:	density of air into vapor	(kg/m^3)
T_l:	temperature of gas	(K)
R:	instantaneous radius of a bubble	(m)
C_l:	specific heat constant of liquid	(J/kgK)
D_{al}:	diffusion coefficient of air into liquid	(m^2/s)
μ_l:	coefficient of viscosity of liquid	(Pa·s)
p_∞:	ambient pressure	(Pa)
σ:	surface tension of liquid	(N/m)

The boundary conditions at gas-liquid interface are expressed as follows.

Temperature on bubble wall:

$$T_g = T_l \tag{14}$$

Condition at saturation:

$$\frac{dp_v}{dT_l} = \frac{Lp_v}{R_v T_l^2} \tag{15}$$

Equality of solubility:

$$p_a = k_H \rho_{al} \tag{16}$$

Equality of mass flux:

$$\rho_g(\upsilon_r - \dot{R}) = \dot{m}_v + \dot{m}_a \tag{17}$$

Equality of heat flux:

$$-\lambda_g \frac{\partial T_g}{\partial r} + L\dot{m}_v = -\lambda_l \frac{\partial T_l}{\partial r} \tag{18}$$

Equality of relative mass flux:

$$-D_{av}\rho_g \frac{\partial}{\partial r}\frac{p_v}{p_g} = j_v = \frac{\rho_a}{\rho_g}\dot{m}_v - \frac{\rho_v}{\rho_g}\dot{m}_a \tag{19}$$

Mass flux diffusion of air into surrounding fluid:

$$-D_{al}\frac{\partial \rho_{al}}{\partial r} = j_{al} = \dot{m}_{al} \tag{20}$$

where

L: latent heat of vaporization (J)
k_H: Henry constant (Pa·m^3/kg)
j_{al}: diffusion mass flux of air into liquid (kg/m^{2}s)
m_a, m_v: condensation mass flux of residual gas in a bubble, vapor (kg/m^{2}s)

Equations for the corresponding physical variation f, such as υ_r, p_g, p_v, p_a, and h_g, can be estimated by first-order linear approximation ($f = f_0 + f'$, where f_0 is a constant equilibrium value, $f' \ll f_0$ is a small variation). These linearized equations and boundary conditions are given in Appendix A. Next, all of the fluctuating variables $f'(\boldsymbol{r}, t)$ are oscillated by the same frequency ω ($f'(\boldsymbol{r}, t)A_f(\boldsymbol{r})e^{j\omega t}$). The eigenvalues are obtained from linear differential equations with constant coefficients for $A_f(\boldsymbol{r})$. Since $A_f(\boldsymbol{r})$ is expressed by the linear summation of the eigenfunctions corresponding to these eigenvalues, the constant coefficients used in the linear combination are calculated from linear algebraic equations by using above the boundary conditions. Consequently, complex amplitude $A_f(\boldsymbol{r})$ is solved as a function of $\boldsymbol{r}$.

3.2. Profiles of Temperature, Partial Pressure of Vapor, and Partial Pressure of Air in an Oscillating Bubble

Temperature fluctuations are rarely seen in the liquid (side) as the surrounding liquid has a large heat capacity, but heat is transferred between the interior of the bubble and surrounding fluid by the contraction and expansion of the bubble. Accordingly, phenomena in the interior of the bubble are shown here.

Figure 3 shows the amplitudes of the fluctuation profiles of the temperature, partial pressure of vapor, and partial pressure of air for 40 kHz ultrasonic irradiation. Temperature fluctuations rarely occur in the liquid (side), and accordingly, the temperature fluctuation $|A_{T_g}|/T_{g0}$ decreases near the bubble wall and becomes zero on the bubble wall. Here, the real amplitude of the gas temperature must be obtained by $|A_{T_g}|$ since A_{T_g} is complex. The saturated vapor pressure on the bubble wall ($R/R_0 = 1$) is held nearly constant, and accordingly, the fluctuation of vapor pressure $|A_{P_v}|/P_{g0}$ decreases near the bubble wall, and becomes zero on the bubble wall like the temperature fluctuation. The vapor diffusion and other effects occur by the evaporation and condensation at the interface, since the temperature distribution exists in the bubble by the oscillation and the saturated vapor pressure on the bubble wall is held constant, these affect the bubble oscillation.

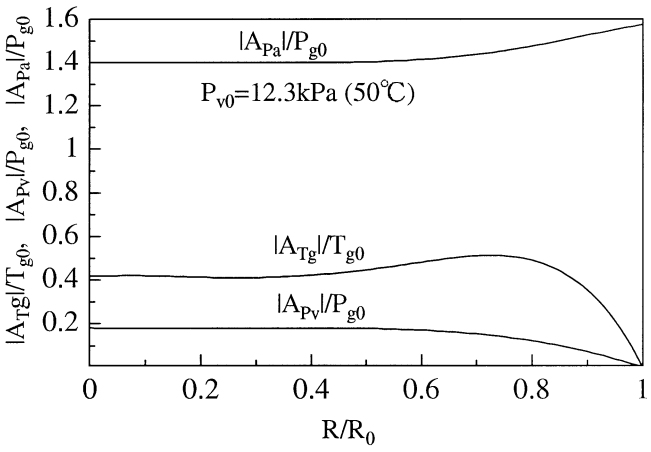

Fig. 3 Amplitude of temprature and partial pressure of air and vapor.

3.3. Damped Oscillation of a Single Free bubble

In order to study how interior phenomena affect the oscillation of a bubble, we obtain the logarithmic decrement (per cycle) of the bubble in free oscillation. When the pressure far from the bubble p_∞ is set to zero, complex angular frequency ω is calculated from linear homogeneous equations. Hence, the damping factor per cycle γ is expressed by multiplying 2π by the ratio of the imaginary part to the real part of complex ω.

$$\gamma = 2\pi \frac{\Im[\omega]}{\Re[\omega]} \tag{21}$$

Figure 4 shows a calculated logarithmic decrement result with a variation of vapor pressure in a bubble. The abscissa is the radius of the single bubble R_0. The logarithmic decrement has a peak value when R_0 is equal to 20 μm, and it increases with vapor pressure.

Figure 5 shows a calculated logarithmic decrement result when the diffusion rate of the air in a bubble into the surrounding fluid is varied. When the diffusion coefficient D_{al} becomes larger and R_0 becomes smaller down to several mm, the influence by the diffusion rate becomes larger.

Figure 6 shows a calculated logarithmic decrement

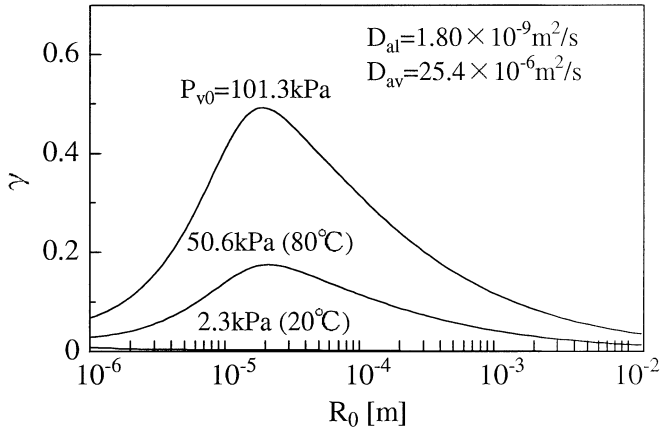

Fig. 4 Effect of partial pressure on the decay of

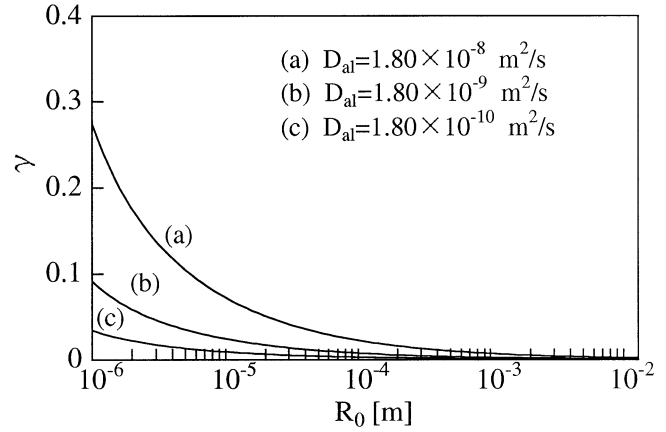

Fig. 5 Diffusion on the decay of bubble oscillation.

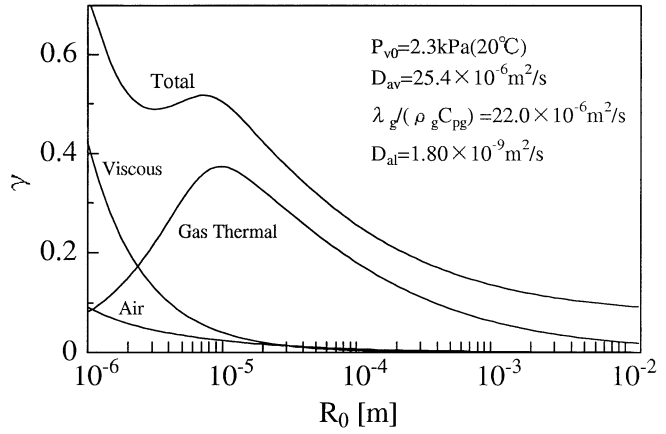

Fig. 6 Bubble oscillation in the normal state.

result under normal temperature and normal pressure. The partial pressure of vapor in the bubble under normal temperature and normal pressure is 2 kPa, and the influence of vapor diffusion on the bubble oscillation is almost negligible. The influence of the thermal diffusion of gas is large when R_0 is nearly 10 μm. The maximum value of the logarithmic decrement is nearly 0.4. When R_0 becomes smaller, the influence of the viscosity of liquid and the diffusion of air into the surrounding liquid becomes larger.

In the cleaning vessel used in the present experiment, it is assumed that a large number of cavitation bubbles with a radius of 50 μm (= 0.05 mm) are generated in the ultrasonic field with a frequency of 40 kHz. As Fig. 6 indicates, the thermal diffusion within the bubble plays a dominant role when the bubble radius is 50 μm. The same result was given by the analysis of Chapman *et al.* [5] which neglected the diffusion of gas and liquid.

3.4. Energy Dissipation of Bubbles in the Vessel by Forced Oscillation

To obtain the actual pressure, the energy loss in the water vessel must be determined. The cavitation bubbles come to suffer forced oscillation when ultrasonic vibration is applied. When the distribution of the corresponding physical quantity in the radial direction can be found by solving the basic equation, the energy dissipation can be calculated [6]. If the energy dissipation $\dot{E}_1$ by the oscillation of a single bubble, is made to occur by only the thermal diffusion, the following equation can be induced [6].

$$\overline{\dot{E}_1} = \frac{\lambda_g}{T_0}\overline{\int_0^{R_0}\left(\frac{\partial T'}{\partial r}\right)4\pi r^2 dr} \tag{22}$$

where T_0 is the average temperature and $^-$ represents an average over one period. The energy dissipation versus frequency when the bubble radius is 50 μm is shown in Fig. 7. A large dissipation occurs at the resonant frequency of the bubbles.

Total energy dissipation $\overline{\dot{E}}$ by bubbles in a cleaning vessel is calculated by multiplying the energy dissipation for a single bubble by bubble density N and integrating over the volume of water V in the cleaning vessel.

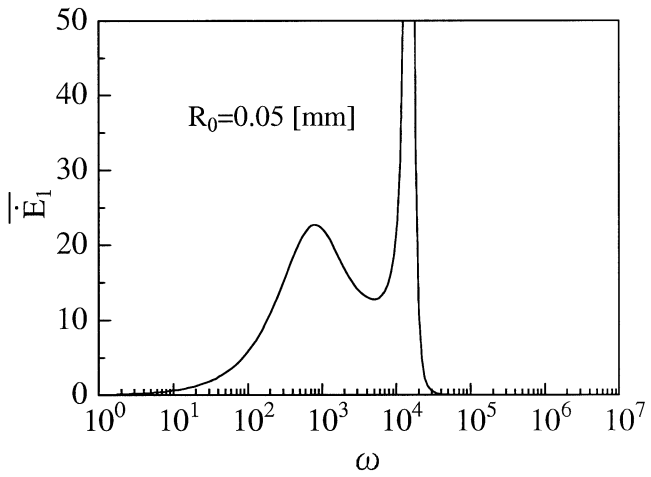

Fig. 7 Energy dissipation.

$$\overline{\dot{E}} = \int_V N\overline{\dot{E}_1}dV \tag{23}$$

Hence, the actual sound pressure can be found by making this dissipation equal to the ultrasonic output. Accordingly, velocity υ_n of the vibrating surface can be obtained from ultrasonic power $\overline{\dot{E}}$ by evaluating the energy dissipation of the bubble oscillation,

$$(2\pi\rho c\upsilon_n)^{-2} = \frac{\pi(\kappa-1)^2 T_0 {R_0}^2\sqrt{2\lambda_g\rho_g\kappa c_{vg}\omega}NV}{\kappa^2 {p_0}^2\overline{\dot{E}}} \cdot \frac{{\omega_n}^4}{({\omega_n}^2-\omega^2)^2+(2\zeta\omega_n\omega)^2} \cdot \frac{1}{V}\int_V\{p^2\}dV. \tag{24}$$

where

$$\omega_n = \sqrt{\frac{3\kappa p_0}{\rho {R_0}^2}}, \quad 2\zeta\omega_n = \frac{4\mu}{\rho {R_0}^2}$$

κ: ratio of specific heat
c_{vg}: specific heat at a constant volume of gas (J/kgK)
ω: angular frequency (rad/s)

p^2 in the integrated function is the square of the non-dimensional sound pressure in Eq. (1). The detailed derivation of Eq. (24) is described in Refs. [7] and [8]. If $\overline{\dot{E}}$ is equal to the ultrasonic output and the profile of the sound field is known, the velocity of the vibrating surface can be determined by giving cavitation bubble radius R_0 and bubble density N.

4. RESULTS OF ANALYSIS

4.1. Sound Profile on the Block Surface

As the ultrasonic wavelength in water at the frequency of 40 kHz is 37 mm, a numerical analysis is carried out by setting the width of the two-dimensional cleaning vessel to 10 wavelengths, and the height to four wavelengths. The pressure or the pressure gradient of the boundary element is obtained by dividing a boundary of the cleaning vessel $2 \times (370 + 148)$ mm into 420 elements (the line segment length of the element is equal to 1/15 the wavelength). Then, the pressure in the cleaning vessel is calculated. Cavitation bubble radius R_0 is 0.05 mm and bubble density N is 1×10^7 #/m^3 by referring the number density [9] of bubble nuclei as reported in experiments measuring bubble nuclei. The electric input power of the transducer is 600 W, but as the transformation efficiency of the ultrasonic transducer employed is 50%, the mechanical output of the transducer becomes 300 W. Velocity υ_n of the vibrating surface is determined so that the energy dissipation is equal to the output power of the transducer.

Figure 8 shows a two-dimensional isobar diagram of standing vibration in a cleaning vessel when the height from the vibrating surface to the base of the block is one wavelength (1λ: about 37 mm). The isobar space in the figure is 0.1 MPa. The standing vibration causes resonance at the base of the block and the pressure becomes high there, in contrast, the pressure is low at the sides and other points in the vessel. Figure 9 shows mean values of the sound pressure at the base of the block, with varying distance y_b from the oscillator. The vertical line in the figure corresponds to Fig. 8. The resonance phenomena appear with a period of about 20 mm.

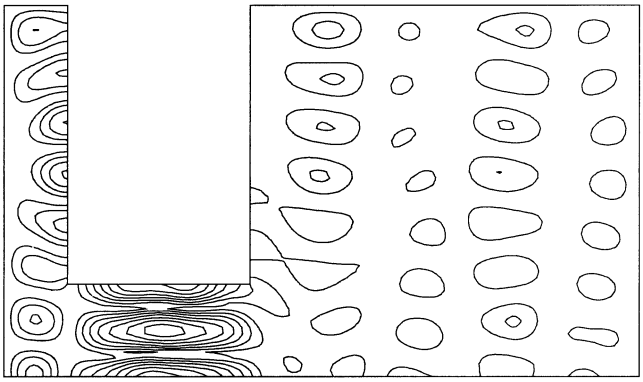

Fig. 8 Isobar diagram in a cleaning vessel, $le = 4\lambda$.

4.2. Water Depth and Cavitation Bubbles

The ultrasonic pressure in a cleaning vessel is governed by the attenuation of the ultrasonic vibration in the vessel. Figures 10 and 11 show analysis results when the depth (*le*) of water filled in the cleaning vessel is made two wavelengths and six wavelengths. The distance from the vibrating surface to the base is one wavelength in each case. In Fig. 10 strong resonance of the standing vibration can be seen, but when the depth of water is six wavelengths, no definite resonant appearance can be seen and the sound escapes around the block.

In order to show this in detail, the mean sound pressure

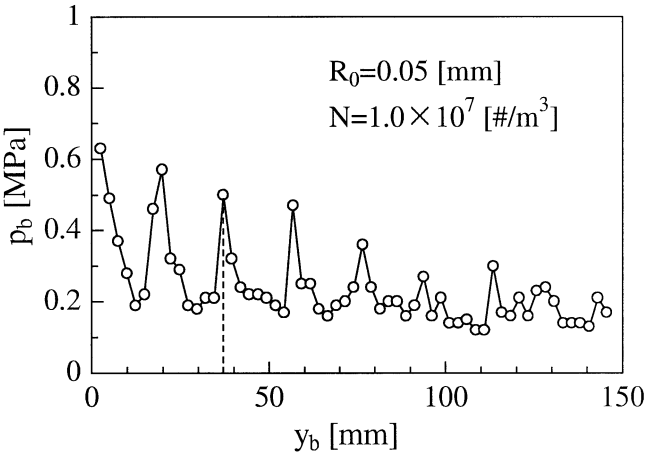

Fig. 9 Pressure on the base of an object, $le = 4\lambda$.

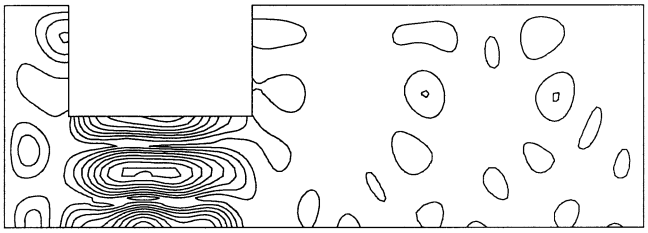

Fig. 10 Isobar diagram in a cleaning vessel, $le = 2\lambda$.

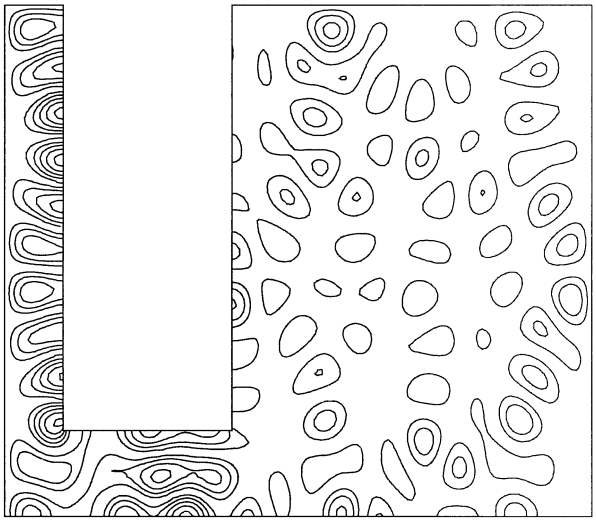

Fig. 11 Isobar diagram in a cleaning vessel, $le = 6\lambda$.

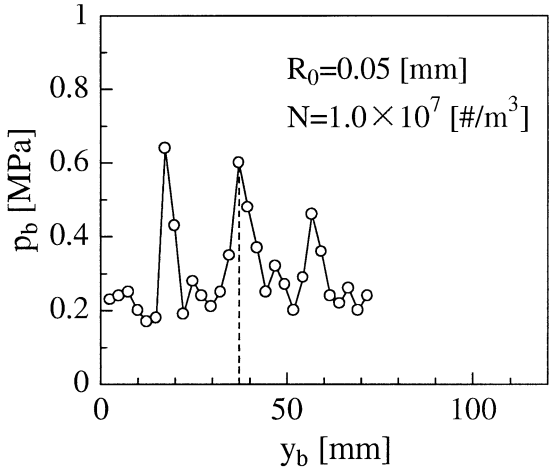

Fig. 12 Pressure on the base of an object, $le = 2\lambda$.

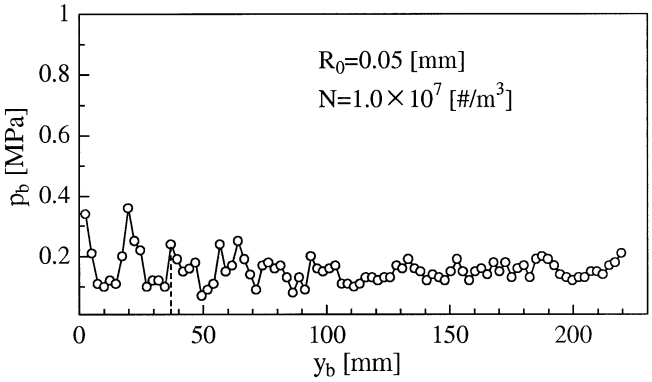

Fig. 13 Pressure on the base of an object, $le = 6\lambda$.

when the height of the block y_b is varied is shown in Figs. 12 and 13. As the depth of water becomes higher, the number of bubbles increases and so a larger attenuation of the ultrasonic vibration occurs. If we compare the case that the depth of water is two wavelengths with the case that it is four wavelengths as in Fig. 8, there is no large difference in the analyzed sound pressure. When the standing wave causes resonance between the ultrasonic generator and the block surface, the sound pressure at the base is independent of the water volume in the cleaning vessel. It is assumed that in the resonant state, only the bubbles that exist between the generator and the block surface oscillate and energy dissipation is caused.

On the other hand, when the depth of the water is large up to six wavelengths, the resonant part becomes irregular and the sound pressure is decreased. When the standing wave causes resonance between the ultrasonic generator and the block surface, the sound pressure becomes lower as the quantity of water in the ultrasonic field increases. The amount of energy dissipation of the ultrasonic wave increases proportionally to the number of bubbles.

5. MEASURED CAVITATION INTENSITY

In order to verify the analyzed sound pressure, the strength of cavitation on the block surface is measured experimentally. The cleaning power by ultrasonic vibration can be evaluated with the mass loss of an aluminum sheet. An aluminum sheet of 15 μm is cut to the size of the bottom area of the block, 105 mm $\times$ 105 mm, and it is stretched to remove any air trapped between the base surface of the block and itself, and after that, the sheet is attached by putting double-face adhesive tape on the four corners of the base. The aluminum sheet immersed in the cleaning vessel is eroded by cavitation damage [1,10]. The mass loss calculated from the eroded area of the aluminum sheet increases linearly under the applied time of less than 50 s. The strength of the cavitation is determined quantitatively as the cavitation intensity (C.I.) by the mass loss rate, where the mass loss is divided by the applied time.

Figure 14 shows the cavitation intensity at the base surface for the depth of four wavelengths. A resonant state appears periodically, and this tendency agrees well with analysis results. Figure 15 shows the same for the depth of water of two wavelengths, the profile of the cavitation intensity is almost the same as that at four wavelengths. In Fig. 16 where the depth is six wavelengths, the resonance comes to have an irregular period and its magnitude

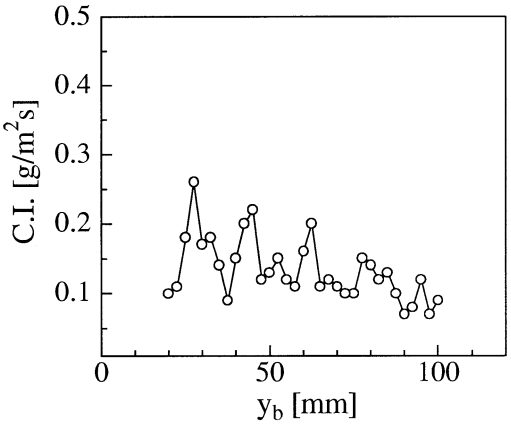

Fig. 14 Cavitation intensity, $le = 4\lambda$.

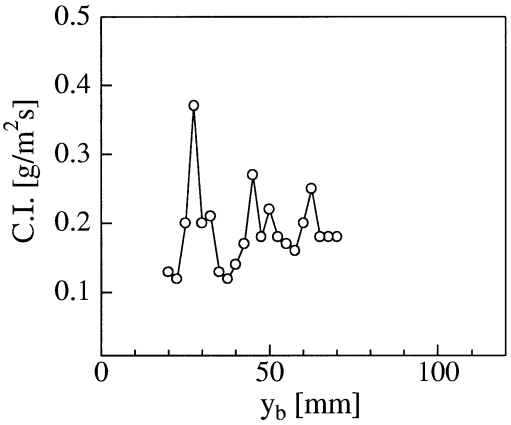

Fig. 15 Cavitation intensity, $le = 2\lambda$.

decreases. These series of measurement results of the cavitation intensity can be well predicted by the present analysis. Hence, the present analysis can predict the cleaning effect by ultrasonic vibration.

6. CONCLUSION

The sound pressure on a block and the pressure profile in a cleaning vessel are analyzed by a boundary element method while varying the water volume in the ultrasonic cleaning vessel. The conclusion of the present paper is shown in the following.

(1) In an ultrasonic field with a frequency of 40 kHz, energy dissipation by thermal diffusion in a bubble is predominant for the dissipation of the oscillation of cavitation bubbles.

(2) The sound pressure can be evaluated well by considering of the thermal diffusion in the bubble by bubble oscillation.

(3) When the standing wave does not cause resonance between the ultrasonic generator and the block surface, the sound pressure on the block surface decreases with increasing water volume.

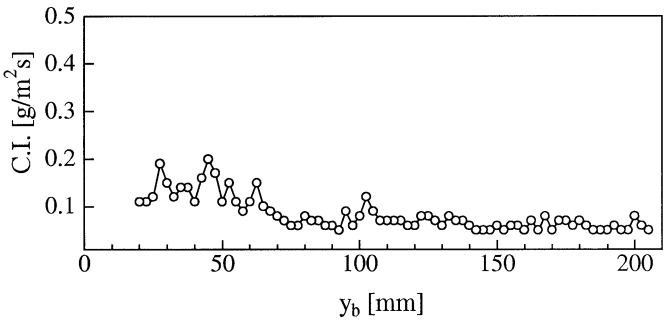

Fig. 16 Cavitation intensity, $le = 6\lambda$.

(4) When the standing wave does cause resonance, in contrast, the sound pressure on the block surface is independent of the water volume in the cleaning vessel. Energy dissipation by bubble oscillation occurs only between the generator and the block base.

REFERENCES

[1] S. Nomura and M. Nakagawa, "Ultrasonic enhancement of heat transfer on narrow surface", *Heat Transfer Jpn. Res.* **22**, 546–558 (1993).

[2] S. Nomura, K. Murakami, Y. Aoyama and J. Ochi, "Effect of changes of frequency of ultrasonic vibrations on heat transfer", *Heat Transfer Asian Res.* **29**, 358–372 (2000).

[3] T. Tanaka, "Sound field analysis by using boundary element method", *J. Acoust. Soc. Jpn.* (*J*) **48**, 229–230 (1992) (in Japanese).

[4] M. Fukuda, T. Murai and Y. Kagawa, "Transient acoustic field analysis by a boundary element model—Two dimensional case", *Proc. 12th Int. Conf. Boundary Elements in Engineering, Sapporo*, Vol. 2, 193–202 (1990).

[5] R. B. Chapman and M. S. Plesset, "Thermal effects in the free oscillation of gas bubbles", *Trans. ASME J. Basic Eng.* 373–376 (1971).

[6] L. D. Landau and E. M. Lifshitz, *Fluid Mechanics* (Pergamon Press, Oxford, 1959), p. 299.

[7] S. Nomura, M. Nakagawa and K. Murakami, "Cavitation intensity and sound pressure on heating elements in an ultrasonic field", *Proc. 9th Int. Symp. Transport Phenomena in Thermal-Fluid Engineering, Singapore*, Vol. 2, 855–860 (1996).

[8] S. Nomura and M. Nakagawa, "Prediction of cavitation intensity by numerical analysis in an ultrasonic field", *J. Acoust. Soc. Jpn.* (*J*) **52**, 592–598 (1996) (in Japanese).

[9] F. B. Petrson, F. Danel, A. Keller and Y. Lecoffre, "Comparative measurement of bubble and particulate spectra by three optical methods", *14th Int. Towing Tank Conf. 1975 Report of Cavitation Committee*, Appendix 1, 27–52 (1975).

[10] S. Nomura and M. Nakagawa, "Cavitation intensity and heat transfer on bottom surface by applying ultrasonic vibration", *Trans. Jpn. Soc. Mech. Eng. B*, **59**-562, 2028–2034 (1993) (in Japanese).

APPENDIX A: LINEARIZED GOVERNING EQUATION

By substituting

$$
\begin{aligned}
&\upsilon_r = 0 + \upsilon_r' \\
&p_{\mathrm{g}} = p_{\mathrm{g}0} + p_{\mathrm{g}}', \quad \rho_{\mathrm{g}} = \rho_{\mathrm{g}0} + \rho_{\mathrm{g}}' \\
&p_{\mathrm{v}} = p_{\mathrm{v}0} + p_{\mathrm{v}}', \quad \rho_{\mathrm{v}} = \rho_{\mathrm{v}0} + \rho_{\mathrm{v}}' \\
&p_{\mathrm{a}} = p_{\mathrm{a}0} + p_{\mathrm{a}}', \quad \rho_{\mathrm{a}} = \rho_{\mathrm{a}0} + \rho_{\mathrm{a}}' \\
&h_{\mathrm{g}} = h_{\mathrm{g}0} + h_{\mathrm{g}}'
\end{aligned} \tag{A·1}
$$

into the physical variable of each fundamental equation in section 3.1, Eqs. (5)–(13) can be linearized.

Omitting small quantities of the second order (f' being of the first order), linearized equations are obtained in the vapor phase.

Continuity equation:

$$
\frac{\rho_{\mathrm{a}0}}{\rho_{\mathrm{g}0} p_{\mathrm{a}0}} \frac{\partial p_{\mathrm{a}}'}{\partial t} + \frac{\rho_{\mathrm{v}0}}{\rho_{\mathrm{g}0} p_{\mathrm{v}0}} \frac{\partial p_{\mathrm{v}}'}{\partial t} - \frac{1}{T_{\mathrm{g}0}} \frac{\partial T_{\mathrm{g}}'}{\partial t} + \frac{1}{r^2} \frac{\partial}{\partial r} r^2 \upsilon_r' = 0 \tag{A·2}
$$

Momentum equation:

$$
\rho_{\mathrm{g}0} \frac{\partial \upsilon_r'}{\partial t} = -\frac{\partial p_{\mathrm{a}}'}{\partial r} - \frac{\partial p_{\mathrm{v}}'}{\partial r} \tag{A·3}
$$

Energy equation:

$$
\rho_{\mathrm{g}0} \frac{\partial h_{\mathrm{g}}'}{\partial t} - \frac{\partial p_{\mathrm{a}}'}{\partial t} - \frac{\partial p_{\mathrm{v}}'}{\partial t} = \lambda_{\mathrm{g}} \ \mathrm{div\ grad}\ T_{\mathrm{g}}' \tag{A·4}
$$

where

$$
\begin{aligned}
h_{\mathrm{g}}' = {} & \frac{M_{\mathrm{a}} C_{p\mathrm{a}} T_{\mathrm{g}0}}{M_{\mathrm{a}} p_{\mathrm{a}0} + M_{\mathrm{v}} p_{\mathrm{v}0}} p_{\mathrm{a}}' + \frac{M_{\mathrm{v}} C_{p\mathrm{v}} T_{\mathrm{g}0}}{M_{\mathrm{a}} p_{\mathrm{a}0} + M_{\mathrm{v}} p_{\mathrm{a}0}} p_{\mathrm{v}}' + C_{p\mathrm{g}0} T_{\mathrm{g}}' \\
& - C_{p\mathrm{g}0} \frac{M_{\mathrm{a}} p_{\mathrm{a}}'}{M_{\mathrm{a}} p_{\mathrm{a}0} + M_{\mathrm{v}} p_{\mathrm{v}0}} T_{\mathrm{g}0} - C_{p\mathrm{g}0} \frac{M_{\mathrm{v}} p_{\mathrm{v}}'}{M_{\mathrm{a}} p_{\mathrm{a}0} + M_{\mathrm{v}} p_{\mathrm{v}0}} T_{\mathrm{g}0}
\end{aligned} \tag{A·5}
$$

Then,

$$
C_{p\mathrm{g}0} = \frac{p_{\mathrm{v}0} M_{\mathrm{v}} C_{p\mathrm{v}} + p_{\mathrm{a}0} M_{\mathrm{a}} C_{p\mathrm{a}}}{M_{\mathrm{a}} p_{\mathrm{a}0} + M_{\mathrm{v}} p_{\mathrm{v}0}}. \tag{A·6}
$$

Equation of diffusion:

$$
\begin{aligned}
& \frac{1}{p_{\mathrm{v}0}} \frac{\partial^2 p_{\mathrm{v}}'}{\partial t^2} - \frac{1}{T_{\mathrm{g}0}} \frac{\partial^2 T_{\mathrm{g}}'}{\partial t^2} - \frac{1}{\rho_{\mathrm{g}0}} \ \mathrm{div\ grad}\ (p_{\mathrm{a}}' + p_{\mathrm{v}}') \\
& \quad = \frac{D_{\mathrm{va}} \rho_{\mathrm{g}0} M_{\mathrm{a}} M_{\mathrm{v}}}{\rho_{\mathrm{v}0} (p_{\mathrm{v}0} M_{\mathrm{v}} + p_{\mathrm{a}0} M_{\mathrm{a}})^2} \\
& \quad \times \left(p_{\mathrm{a}0} \ \mathrm{div\ grad}\ \frac{\partial p_{\mathrm{v}}'}{\partial t} - p_{\mathrm{v}0} \ \mathrm{div\ grad}\ \frac{\partial p_{\mathrm{a}}'}{\partial t} \right)
\end{aligned} \tag{A·7}
$$

In the liquid phase, the following linearized equations are deduced from Eqs. (11), (12), and (13).

Diffusion equation for the liquid phase around the bubble:

$$
\rho_l C_l \frac{\partial T_l'}{\partial t} = \lambda_l \ \mathrm{div\ grad}\ T_l' \tag{A·8}
$$

Diffusion equation of air into liquid:

$$
\frac{\partial \rho_{\mathrm{a}l}'}{\partial t} = D_{\mathrm{a}l} \ \mathrm{div\ grad}\ \rho_{\mathrm{a}l}' \tag{A·9}
$$

Motion of bubble:

$$
\rho_l R_0 \frac{d^2 R'}{dt^2} + \frac{3}{2} \rho_l \left(\frac{dR'}{dt} \right)^2 + \frac{4\mu_l}{R} \frac{dR}{dt} = p_{\mathrm{g}} - p_\infty - \frac{2\sigma}{R} \tag{A·10}
$$

In addition, the linearized boundary conditions are obtained as follows.

$$
\frac{T_{\mathrm{g}}'}{T_{\mathrm{g}0}} = \frac{T_l'}{T_{\mathrm{g}0}} \tag{A·11}
$$

$$
\frac{p_{\mathrm{v}}'}{p_{\mathrm{v}0}} = \frac{L}{R_{\mathrm{v}} T_{\mathrm{g}0}} \frac{T_l'}{T_{\mathrm{g}0}'} \tag{A·12}
$$

$$
p_{\mathrm{a}}' = k_{\mathrm{H}} \rho_{\mathrm{a}l}' \tag{A·13}
$$

$$
\rho_{\mathrm{g}0} (\upsilon_r' - \dot{R}') = \dot{m}_{\mathrm{v}} + \dot{m}_{\mathrm{a}} \tag{A·14}
$$

$$
-\lambda_{\mathrm{g}} \frac{\partial T_{\mathrm{g}}'}{\partial r} + L \dot{m}_{\mathrm{v}} = -\lambda_l \frac{\partial T_l'}{\partial r} \tag{A·15}
$$

$$
\begin{aligned}
\frac{\rho_{\mathrm{a}0}}{\rho_{\mathrm{g}0}} \dot{m}_{\mathrm{v}} - \frac{\rho_{\mathrm{v}0}}{\rho_{\mathrm{g}0}} \dot{m}_{\mathrm{a}} = {} & - \frac{D_{\mathrm{av}} \rho_{\mathrm{g}0} M_{\mathrm{a}} M_{\mathrm{v}}}{(p_{\mathrm{v}0} M_{\mathrm{v}} + p_{\mathrm{a}0} M_{\mathrm{a}})^2} \\
& \times \left(p_{\mathrm{a}0} \frac{\partial p_{\mathrm{v}}'}{\partial r} - p_{\mathrm{v}0} \frac{\partial p_{\mathrm{a}}'}{\partial r} \right)
\end{aligned} \tag{A·16}
$$

$$
-D_{\mathrm{a}l} \frac{\partial \rho_{\mathrm{a}l}'}{\partial r} = m_{\mathrm{a}} \tag{A·17}
$$

Shinfuku Nomura was born in 1964. He received his B.E., M.E., and Dr. Eng. degree from Toyohashi University of Technology, Aich, Japan in 1987, 1989 and 1993, respectively. In 1994, he join the Faculty of Engineering at Ehime University and now he is an Associate Professor. His research interests include the effective utilization of acoustic energy, heat and mass transfer in acoustic field and cavitation bubbles. He is a member of ASJ, Jpn. Soc. Mech. Eng., Heat Transfer Soc. Jpn., and Jpn. Soc. Multiphase Flow.

Masafumi Nakagawa was born in 1948. He received the B.E. degree from Shizuoka University, Shizuoka, Japan, in 1970, his M.E. and Dr. Eng. degrees from Tokyo Institute of Technology, Tokyo, Japan, in 1972 and 1977, respectively. After working at Kawasaki Heavy Industries Co., Tokyo, he is now an Associate Professor of Toyohashi University of Technology, Aich Japan. His research interests include the energy conversion systems and the heat mass transfer of super sonic multiphase flows, using electromagnetic and acoustic feild. He is a member of Jpn. Soc. Mech. Eng., Jpn. Soc. Multiphase Flow, Jpn. Soc. Powder Technology, and Atomic Energy Soc. Jpn.